

Article Info

Received: 20 Feb 2015 | Revised Submission: 25 Feb 2015 | Accepted: 28 Feb 2015 | Available Online: 15 Mar 2015

Thermal Evaporation- Modeling and Microstructure Studies of Indium and Tin Deposition

Shailendra Kumar Gaur and R. S. Mishra***

ABSTRACT

The present work represents the modeling of nano scale tin & indium films by computing the film thickness, mass deposited on the substrate and mass transfer rate with time dependent model using BDF solver. Tin and indium is evaporated from a resistively heated evaporator source at a temperature of 1855 K and 1485 K respectively in a pressure (vacuum) of 100 Pa onto silicon surface held on a fixed surface. The film thickness varies between 144 nm to 164 nm for Tin and 164 nm to 183 nm for Indium across the sample after 60 sec of deposition, with radial symmetry about the midpoint of the source.

The film thickness as well as mass deposited at a point increases linearly with time. Since the angular distribution is of particular interest in this model, by increasing the integration resolution to a maximum value for ensuring the most accurate angular resolution when computing the flux. The surface temperature is required to specifying the temperature of the evaporating tin and indium source using constant elements for turn off the refinement in the post-processing settings. The SEM micrographs of tin and indium at different magnifications shows the 100nm to 1microns grain size along the grain boundaries. Similarly, XRD analysis with $K\alpha$ (wavelength 1.541874) shows the peaks of intensity at different 2θ angles for different orientations of planes with polycrystalline structure.

Keywords: *Physical Vapor Deposition; Modeling; Film Thickness Simulation; Tin Evaporation; Indium Evaporation; Thin Film Deposition.*

1.0 Introduction

Physical methods produce the atoms that deposit on the substrate by evaporation and sputtering. Sometimes called vacuum deposition because the process is usually done in an evacuated chamber. PVD is used for metals while dielectrics can be deposited using specialized equipments. It rely on thermal energy supplied to the crucible or boat to evaporate atoms. Evaporated atoms travel through the evacuated space between the source and the sample and stick to the sample. Few, if any, chemical reactions occur due to low pressure can force a reaction by flowing a gas near the crucible. Surface reactions usually occur very rapidly and there is very little rearrangement of the surface atoms after sticking. Thickness uniformity and shadowing by surface topography, and step coverage are issues. Ali Moarrefzadeh et al. [1] discussed that Physical vapor

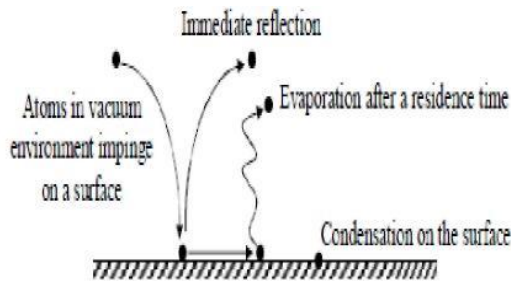
deposition (PVD) includes a wide range of vacuum coating processes in which material is physically taken out from a source by evaporation or sputtering, transported through a vacuum or partial vacuum by the energy of the vapor particles, and condensed as a film on the surfaces of appropriately placed parts or substrates. A group of very versatile coating processes in which a material is converted to its vapor phases in a vacuum chamber and condensed onto a substrate surface as a very thin film (upto 1 micron thickness). The deposition of thin film layers from the vapor phase is done through several methods. We study and analyze the physical vapor deposition (PVD) techniques and equipments that are in common use in the large scale production of coatings that find uses in the optical, display, decorative, tribological, and energy-generating/ saving industries. Evaporating materials are classified as dielectric compounds, metals, alloys, or mixtures. The same

*Corresponding Author: Department of Mechanical, Production & Industrial and Automobiles Engineering, Delhi Technological University, New Delhi, India (E-mail: professor_rsmishra@yahoo.co.in)

**Department of Mechanical, Production & Industrial and Automobiles Engineering, Delhi Technological University, New Delhi, India

evaporant material can exhibit different optical, electrical, and mechanical properties depending on the deposition process. Titanium oxide is a unique example of a metal oxide compound that, depending on deposition process parameters, can be made into film layers that are: transparent, electrically conductive, chemically reactive to light and bio-agents, chemically inert, or exhibit spectrally selective absorption. The dependent parameters are starting composition, oxidation state, and crystalline structure and packing density. PVD techniques used generally are basically two in nature: thermal evaporation by resistively heating or by using an electron-beam heating, and sputtering, a non-thermal process. Alterations and accompaniments are made to the basic PVD techniques to permit different coating materials and substrate types to be included. Process additions designed to alter the growth nano-structure or composition of the film through control of the dependent variables listed above include bombardment of the growing film by high energy inert- or reactive ions, substrate heating, atmosphere composition and partial pressure, rate, and vapor incidence angle. A further important variable contribution to the nucleation and self-assembling growth structure of the condensing atoms, that we have discussed frequently, is the condition both chemical and physical of the substrate surface (PVD process Deposited films are typically evaluated for visual defects, thickness, and adhesion. Visual defects such as bare spots, small voids, incorporated flakes, or debris can be observed with a stereo microscope having a magnification of 10 to 100 times. Film thickness

Fig 1: Mechanism of Thermal Evaporation Process (ref. [1])

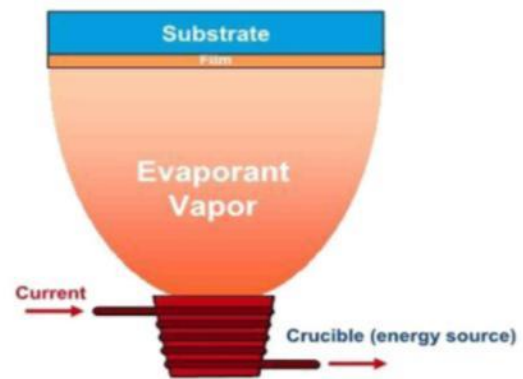


is generally measured by one of the following methods: Thickness of film as modeled can be

simulated experimentally with dektek surface profilometer with diamond size of 12.5 urn radius stylus. Polished metallurgical micro sections are used to microscopically observe the coating thickness on various part surfaces. This method is the most direct way to determine thickness uniformity. Beta (high-energy electron) backscatter instruments are used to measure the film thickness nondestructively.

This is an indirect method that requires calibration with a known standard; substantial errors can be made in measuring the film thickness on curved surfaces if care is not exercised. In thermal evaporation process, load the source material-to-be-deposited (evaporant) into the container (crucible). Then resistively heat the container (tungsten or molybdenum boat) containing source to high temperature i.e. evaporation temperature depending upon the material to be deposited. The source material evaporates and evaporant vapor transports to and impinges on the surface of the substrate. Evaporant condenses on and is adsorbed by the surface.

Fig 2: Thermal evaporation process (ref. CIMS applied physics)



Further study shows that evaporation used in thin film deposition can be done by:

- a) Thermal evaporation
- b) E-beam evaporation

Thermal evaporation is very old, easy, reliable and good method of deposition while E-beam evaporation requires elaborate and complex system. Moreover high velocity electron creates surface defects and stress on the deposited surface. The present work has been performed to achieve the following objectives:

1. To find out the deposited film thickness on the silicon substrate and variation of the thickness across the surface of sample.
2. To find out the mass deposited on the silicon substrate and its variation with time
3. To find out the mass deposition rate on the silicon substrate with time
4. Micrograph and microstructure analysis of the deposited film SEM and XRD for grain size along grain boundaries and orientation of crystal planes for X-ray.

2.0 Literature Review

Thin tin oxide deposited surface is very useful in industries due to their properties such as n-type Semiconductor character, high optical transmission in visible range, high reflectivity; in the infra-red as well as good chemical resistance. Thus they can be used to form transparent and chemically stable thermal barriers.

C. R. Zamarrenoa et al. [3] discussed the fabrication of optical fiber refractometers based on indium tin oxide (ITO) coatings with good sensitivity in the visible spectral region. ITO thin-films have been deposited by using sputtering mechanism and employing a rotating mechanism that makes possible the fabrication of smooth homogeneous coatings onto the optical fiber core. Souad Laghrib et al. [4] discussed the vacuum evaporation of Tin followed by annealing with oxygen flow to obtain Tin oxide thin layers.

He did a lot of experiments by varying the deposited Tin thickness as well as annealing conditions by varying annealing temperature with different duration and found that at high temperature annealing forms nanocrystalline tin oxide. Sea-Way Jan et al.[5] discussed the formation of indium tin oxide by first metal tin and indium deposition in oxygen in vacuum coating system maintain vacuum of 1×10^{-6} torr by combination of rotary and diffusion pump. Further studied the deposited film through XRD, SEM, TEM, Hall measurement and found polycrystalline film with bcc structure. This film is used in front panels in liquid crystal and electroluminescence displays, transparent heating elements, high-efficiency ITO/GaAs and ITO/InP solar cells, blue light electroluminescence etc. D. Bruce Buchholz et al. [6] discussed the few nm thin

layer of indium oxide by pulse layer deposition method and studied formation of crystalline and amorphous with variation of temperature and density variation. Alexandu C. Fechete et al. [7] discussed the indium oxide nanostructures in the form of nanobelts and nanorods with few microns length and 200nm width developed by thermal evaporation on silicon substrates with and without presence of gold catalysts in temperature range of 600- 900° C in which growth process involved are vapor-solid and vapor-liquid-solid and the nanobelts are appx. 10-200 nm wide and few micrometers long at 750°C when no catalyst while when Au catalyst is used, homogenous scattered nanorods obtained at 900°C. C. A. Pan et al. [8] discussed that high quality and high conductive indium oxide films prepared by thermal evaporation from In and In₂O₃ source in vacuum chamber with low pressure of 0.2 of which properties comparable to tin doped indium oxide films. Its low resistivity is as a result of excellent electron mobility ($\sim 70 \text{ cm}^2/\text{V sec}$) though the electron concentration is rather high which makes it a perfect for fabrication of semiconductor device.

Burstein shifts due to high electron density in conduction band also seen. B. Maniscalco et al. [9] discussed the thin film thickness measurement of Indium Tin Oxide made using coherence correlation interferometry. Optical transmission over the whole visible spectra with a steep decrease 380 nm. Indium Tin Oxide(ITO) is widely used in applications such as touch screens, LCD and LED displays, thin film photovoltaics. M.Trzcinski et al [10] discussed the alloy formation of ultrathin Ag and In layers deposited on W(100) starting at room temperature and finished after a small annealing at 600 K.

The alloying process is originally geometrical and no major difference between 2D layered alloys and 3D bulk alloys can be found. Varieties of coatings can be deposited such as metals, alloys, ceramics and other inorganic compounds, and even certain polymers. Deposition can be done onto the varieties of substrates such as metals, glass, and plastics. The properties of atavistically deposited films depend strongly on:

- The material being deposited
- Substrate surface chemistry and morphology
- The surface preparation process
- The details of deposition process and the deposition Parameters :

- mean free path of evaporant
- source to substrate distance
- vapour pressure of evaporant
- sticking coefficient

Condensation and nucleation- Atoms that impinge on a surface in a vacuum environment may be reflected immediately, re-evaporate after a residence time, or condense on the surface shown in figure

1. Mean free path is the minimum distance between two successive collisions and is given by formula depending on the vacuum in the chamber:

$$\lambda = \frac{k_B T_c}{\sqrt{2\pi} \cdot P \cdot d^2}$$

Where T- usually room temp of chamber P- vacuum in chamber based on this mean free path source to substrate distance is optimized for constant flux and better deposited film quality. Vapor pressure varies depending upon the source temperature and is different for different materials, for suitability standard plot [11] is provided from which depending upon source material vapor pressure is selected. Sticking coefficient is defined as the ratio of the condensing atoms to impinging atoms. If the atoms do not immediately react with the surface, they will have some degree of surface mobility over the surface before they condense. Re-evaporation is a function of bonding energy between the adatom and the surface, the surface temperature, and the flux of mobile adatoms e.g. the deposition of cadmium on a steel surface having a temperature greater than about 200 °C will result in total re-evaporation of the cadmium. The energy of the atom, atom-surface interaction (chemical bonding), and the temperature of the surface influence the capability of an atom on a surface. The mobility on a surface can change because of variations in chemistry or crystallography. The various crystallographic plates of a surface have different surface free energies that influence the surface diffusion. Atoms

condense on a surface by losing energy. They lose energy by:

- Forming and breaking chemical bonds with the substrate atoms.
- Finding preferential nucleation sites (lattice defects, atoms steps, and impurities)
- Interacting with another diffusing surface atoms (same species)

- Colliding or reacting with adsorbed surface species. Atoms form nuclei after condensation. Homogenous

nucleation is said to occur if the surface is of same material as the deposition atoms and if they are different materials, the process is called heterogeneous. In semiconductor field, heterogeneous nucleation forms hetero- junctions. G.H. Gilmer [2] et al discussed that three types of nucleation mechanisms have been identified; they differ according to nature of interaction between the posited atoms and the substrate material.

Frank-Van der Merwe mechanism leading to a monolayer-by-monolayer growth (layer growth; ideal epitaxy). Volmer-Weber (V-W) mechanism, characterized by a three-dimensional nucleation and growth (island growth). Stranski-Krastanov (S-K) mechanism, where an altered surface layer is formed by reaction with the deposited material to generate a strained or pseudomorphic structure, followed by nucleation on this layer (Layer + island growth) nuclei coalescence and agglomeration The nuclei develop by collecting atoms that diffuse over the surface. Isolated nuclei grow laterally and vertically on the surface to form a continuous film and to form a continuous film less amount of material is needed if nucleation density is high.

The principal growth mode of nuclei may be: laterally over the substrate surface (wetting growth) such as gold on copper and chromium, iron on W-O surfaces, and titanium on SiO₂ the nuclei may prefer to grow in a vertical mode (dewetting growth) such as nickel and copper on W-O surfaces, and gold on carbon, Al₂O₃, and SiO₂. Growth and coalescence of the nuclei can leave interfacial voids or structural discontinuities at the interface, particularly if there is no chemical interaction between the nuclei and substrate material and dewetting growth occurs.

Though a lot of research work has been done on the evolution of tin and indium film deposited on nanoscale or higher thickness by different deposition process through different heating sources (resistively, sputtering, E-beam, magnetron, radio frequency) in different baskets/crucibles at different temperatures and modeled mostly with direct simulation monte carlo.

Also these methods solve in the volumes of the modeled and geometries. Number densities found

to be not accurate and precise. Ineligible simulation for the accurate modeling of low pressure, low velocity gas flows in complex geometries. These studies subjected to statistical scatter. Moreover, these could not completely explained free molecular flow interface and applied dsmc computes the trajectories of large numbers of randomized particles through the system, but introduces statistical noise to the modeling process and also the method is slower.

3.0 Experimental Set-up

The island films were prepared using a laboratory thermal evaporation setup working at residual vacuum of $(2.5 - 4) \times 10^{-6}$ mbar.

The deposition setup was equipped with the two-stage vacuum system based on the diffusion pump (oil based), turbo molecular or cry pump along with rotary vane pump or rotary screw pump (oil free). In case of oil based pumps the ultimate vacuum achieved in the system depends upon the vapour pressure of the oil used in pumps, generally Silicone based oils are used to achieve vacuum of 1.0×10^{-6} order in the chamber. Sometimes high discharge Ar gas plasma substrate cleaning can be done at vacuum of 5×10^{-3} mbar, if needed.

The films were deposited on the substrates cleaned in the ultrasound bath in isopropyl alcohol and drained by a compressed air flux. During the deposition, all substrates were kept at room temperature i.e

4.0 Result Analysis

General description of the model is presented in fig. 1 where low pressure gas flow in vacuum system i.e molecular flow and it can be seen that the model inputs are ambient temperature, evaporant temperature, vapour pressure, molecular weight, density of gold, neglecting the substrate surface temperature. The Free Molecular Flow interface uses the angular coefficient method to model flows with Knudsen numbers $Kn > 10$. This physics interface avoids solving the physics in the volumes of the modeled geometries, and requires meshing only of the surfaces. Completely diffuse scattering (total accommodation) and emission are assumed at all surfaces in the geometry, and flow is computed by integrating the flux arriving at a surface from all other surfaces in its line-of-sight. This means that the dependent variables exist only on the surfaces of the geometry, and the solution process is much faster than the DSMC method. Furthermore, it is not subject to statistical scatter. Number densities are reconstructed using a method included in the Free Molecular Flow interface. The Molecular Flow Module is designed to offer previously unavailable simulation capabilities for the accurate modeling of low pressure, low velocity gas flows in complex geometries. It is ideal for the simulation of vacuum systems including those used in semiconductor processing, particle accelerators and mass spectrometers. Small channel applications (e.g. shale gas exploration and flow in nanoporous materials) can also be addressed. The Molecular Flow Module uses a fast angular coefficient method to simulate steady-state free molecular flows. We can model isothermal and nonisothermal molecular flows, and automatically calculate the heat flux contribution from the gas molecules. The discrete velocity method is also included in the module for the simulation of transitional flows. Historically, flows in this regime have been modeled by the direct simulation Monte Carlo (DSMC) method. This computes the trajectories of large numbers of randomized particles through the system, but introduces statistical noise to the modeling process. For low velocity flows, such as those encountered in vacuum systems, the noise introduced by DSMC renders the simulations unfeasible. COMSOL uses alternative approaches: employing a discrete velocity method for transitional

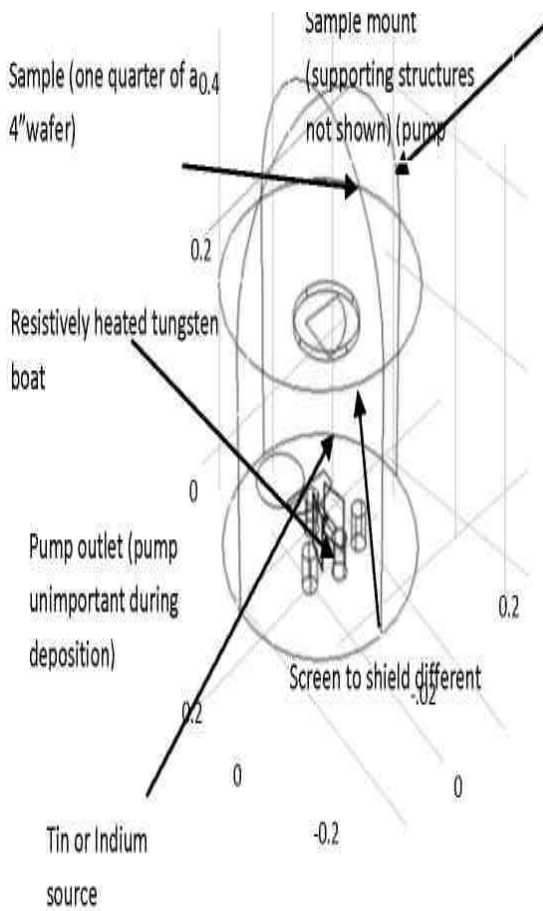
Table 1: Typical Boat /Crucible Material

| Refractory Metals | | |
|-------------------------------------------|--------------------|----------------------------------------------------------------|
| Material | Melting Point (°C) | Temperature for 10-mtorr Vapor Pressure (P _v) (°C) |
| Tungsten (W) | 3380 | 3230 |
| Tantalum (Ta) | 3000 | 3060 |
| Molybdenum (Mo) | 2620 | 2530 |
| Refractory Ceramics | | |
| Graphitic Carbon (C) | 3799 | 2600 |
| Alumina (Al ₂ O ₃) | 2030 | 1900 |
| Boron Nitride (BN) | 2500 | 1600 |

flows (using a Lattice Boltzmann velocity quadrature) and the angular coefficient method for molecular flows. Using the input parameters, the model computes the thickness of gold deposited, mass deposited on the surface of substrate, mass transfer rate and mass loss by using COMSOL software. The following wall conditions are inbuilt in COMSOL software:

wall, out gassing wall, adsorption/desorption, deposition. In adsorption/desorption boundary condition, sticking coefficient can be defined along with other condition. Tin and Indium is placed in resistively heated Tungsten boat which is having very high melting point of 3420° C. Substrate is one quarter of a 4" wafer mounted on stationary support on top of tungsten boat depending upon the mean free path and Langumuire-Kundsens relation. A screen is placed to cover the substrate, if more than one source is used.

Fig 3: Model Geometry Various Components of evaporator



The basic governing equation for depositing molecular flux on the surface is Langmuire-Knudsen Relation which shows the mass deposition rate per unit area of source surface:

$$R_m = C_m \left(\frac{M}{T} \right)^{\frac{1}{2}} \cos \theta \cos \phi \frac{1}{r^2} (P_e(T) - P)$$

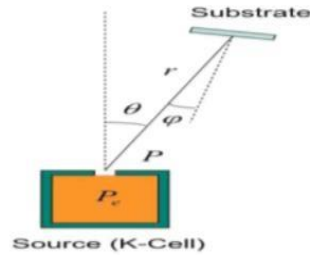


Fig. 4. Source to Substrate Geometry

- $C_m = 1.85 \times 10^{-2}$
- r : source-substrate distance (cm)
- T : source temperature (K)
- P_e : evaporant vapor pressure (torr), function of T
- P : chamber pressure (torr)
- M : evaporant gram-molecular mass (g)

Uniformity on a Flat Surface

Consider the deposition rate difference between wafer center and edge:

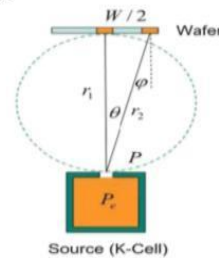


Fig. 5. Source to Flat Surface Geometry

$$R_1 \propto \frac{1}{r_1^2}$$

$$R_2 \propto \frac{1}{r_2^2} \cos^2 \theta = \frac{r_1^2}{r_2^4}$$

Define Uniformity:

$$\sigma(\%) = \frac{R_1 - R_2}{R_1} (\%)$$

$$\sigma = 1 - \left(1 + \left(\frac{W}{2r_1} \right)^2 \right)^{-2} \approx \frac{W^2}{2r_1^2} \quad \text{or} \quad \frac{W}{r_1} = \sqrt{2\sigma}$$

5.0 Results & Discussion

In table 2 & 3 various input parameters required for the tin and indium models are given to compute the molecular flow in vacuum system.

Generally, the ambient temperature is fixed based on the experimental setup or experimental conditions but the evaporation temperature can be varied as per the thickness or mass transfer to be deposited on the substrate. This evaporation temperature can be increased or decreased depending considering the vapour pressure, to make fast the mass transfer keeping the good adhesion with uniformity on the substrate surface.

In table 2 &3 various input parameters required for the tin and indium models are given to compute the molecular flow in vacuum system. Generally, the ambient temperature is fixed based on the experimental setup or experimental

conditions but the evaporation temperature can be varied as per the thickness or mass transfer to be deposited on the substrate. This evaporation temperature can be increased or decreased depending considering the vapour pressure, to make fast the mass transfer keeping the good adhesion with uniformity on the substrate surface.

Table 2: Input Parameter for the tin Model

| Name | Expression | Value | Description |
|-------|------------------------|--------------------------|-------------------------|
| Tamb | 293.15[K] | 293.2 K | Ambient temperature |
| Tevap | 1855[K] | 1855 K | Evaporation temperature |
| pvap | 100[Pa] | 100.00 Pa | Vapor pressure of Tin |
| Mn0 | 118.71[g/mol] | 0.11871kg/mol | Molecular weight of Tin |
| Rho0 | 7.36 g/cm ³ | 7.36E3 kg/m ³ | Density of Tin |

Table 3: Input Parameters for the Indium Model

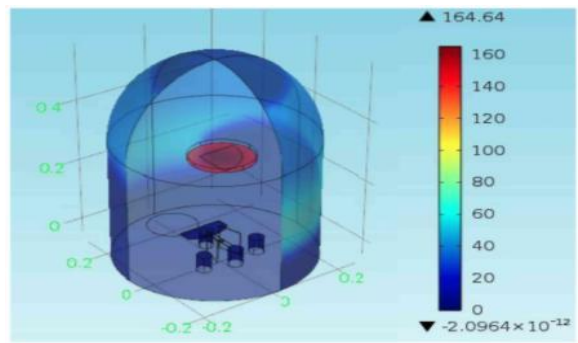
| Name | Expression | Value | Description |
|-------|------------------------|--------------------------|----------------------------|
| Tamb | 293.15[K] | 293.2 K | Ambient temperature |
| Tevap | 1485 [K] | 1485 K | Evaporation temperature |
| pvap | 100[Pa] | 100.00 Pa | Vapor pressure of indium |
| Mn0 | 114.818[g/mol] | 0.1148 kg/mol | Molecular weight of indium |
| Rho0 | 7.31 g/cm ³ | 7.31E3 kg/m ³ | Density of indium |

Figure 6 shows the flux of tin molecules on the surfaces of the model. This constant flux determines the thickness of Tin deposited shown in figure. In figure 7, it is obvious the tin film thickness is maximum in the centre of substrate positioned directly on vertically centre of tungsten boat/source, greater than 164 nm after 60 seconds of thermal evaporation process. This thickness decreases radially outwards surface of the substrate to 144 nm. In Figure 8 based the molecular flux deposited on substrate, graph shows the tin deposited thickness after 60 seconds from initial condition of zero second. It is clear from graph that the film thickness varies linearly with time. In figure 9 graph is plotted with time for mass (kg x E-6) deposited on the surface of substrate and shows that mass deposited on substrate increases with time as in the case of figure 8 since the depositing thickness with time adds mass also on the substrate.

In figure 10 mass transfer rate (kg x E-8/sec) is plotted for 60 seconds and is a straight constant abscissa parallel line.

Time = 60 Surface Film thickness (nm)

Fig 6: Tin Film Deposited Thickness



Time = 60 sec Surface: film thickness (nm)

Fig 7: Variation of Deposited tin Film Thickness Across the Surface

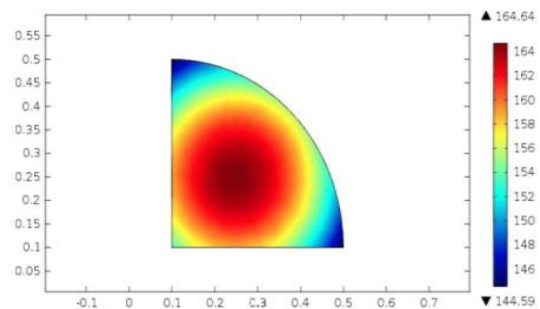


Fig 8: Film Thickness vs Time at a Point on the Corner of the Sample

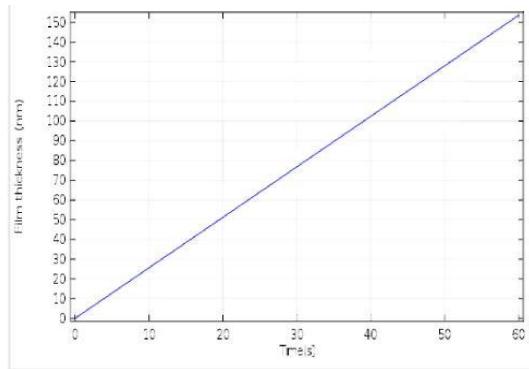


Fig 9: Mass of Tin Deposited on the Surface

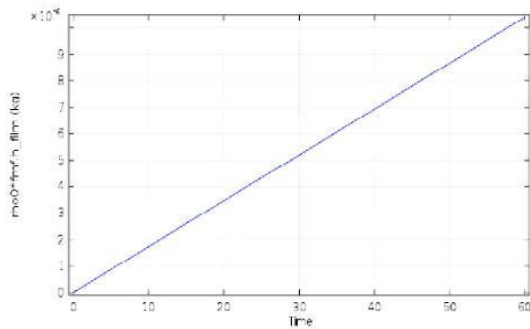


Fig 10: Variation of Mass Transfer Rate of tin with Time

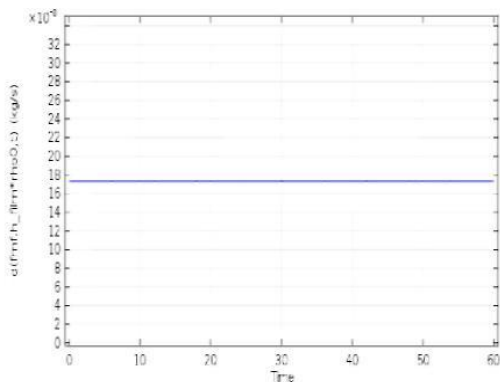


Figure 11 shows the deposition of indium at 100 Pa with evaporation temperature of 1485 K. The maximum film thickness achieved is 183 nm, this film thickness may vary by varying the evaporation temperature with time and vapor pressure. Similarly, the indium thin film thickness varies from 160 to

183 nm from the centre of substrate to outer surface and it is maximum at the centre as shown in figure 12.

Time = 60 sec Surface film thickness (nm)

Fig 11: Indium Film Deposited Thickness

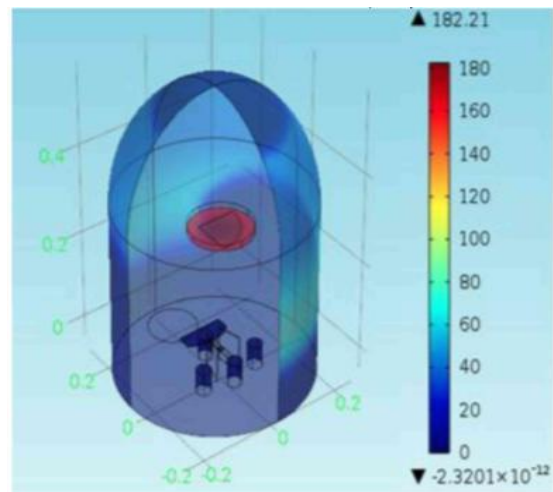


Fig 12: Variation of Deposited Indium Film Thickness Across the Surface

Time=60 Surface: Film thickness (nm)

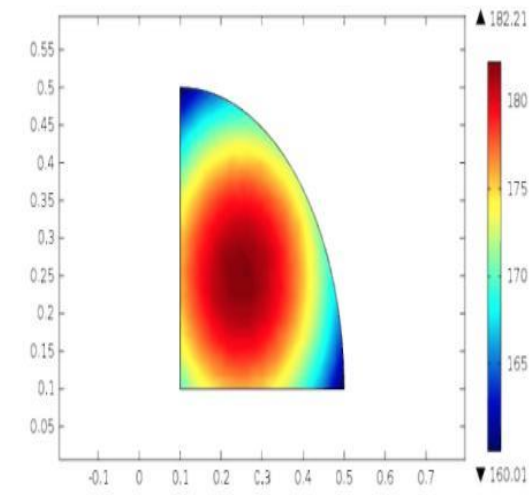


Figure 13 shows the variation of thickness at a point on the surface and its variation with time i.e after 60 sec from zero to 183nm. This plot is taken at present at the edge of substrate and similarly by selecting the another point on the surface, we can find similar plot.

Fig 13: Film Thickness vs Time at a Point on the Corner of the Sample

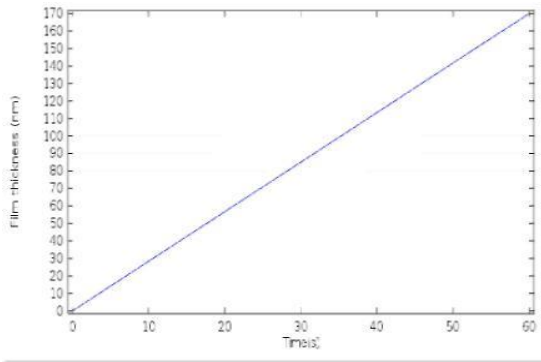


Fig 14: Mass of Indium Deposited on the Surface

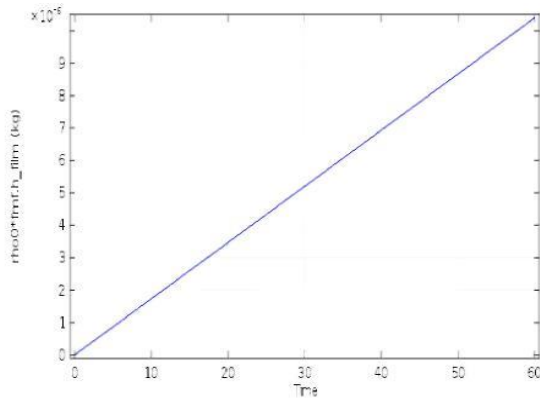


Figure 14 shows the mass (kg x E- 6) of indium deposited on the surface of substrate and shows that as mass deposited on substrate increases with time. Now as in the case of figure 13 where the depositing thickness with time adds, mass also on the substrate deposited increases.

Fig 15: Variation of Mass Transfer Rate of Indium with Time

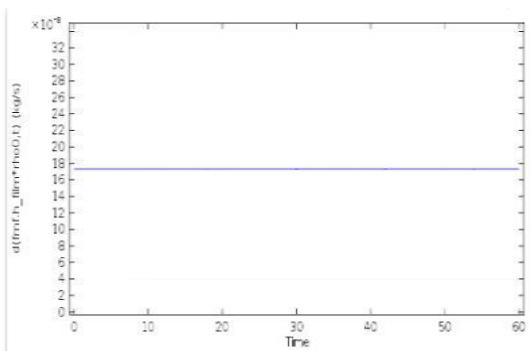


Figure 15 shows mass transfer rate (kg x E- 8/sec) is plotted for 60 seconds and is a straight constant abscissa parallel line. Only the flux is required to compute the deposition rate, but in this instance, since most of the computational time is used to compute the view factors, solving the time dependent problem adds little additional time to the solution process. Using a time dependent model also allows for more advanced extensions of the model, for example, re-evaporation of gold from hot surface close to the evaporative source could be included. Definitely there is loss of source material during thermal evaporation since only a fraction of the material is deposited on the surface while we are evaporating a large quantity of it. The SEM micrographs shown in figure 16, 17 are at 5KX, 10KX magnifications while fig. 18, 19 are at 25KX magnification, 20KV Extra High Tension (EHT), working distance 10.6mm to go through better study and analysis of grain size and structure. The SEM revealed the growth of 200nm-1µm grains size.

Fig 16: SEM Micrographs of tin at 5X Magnification

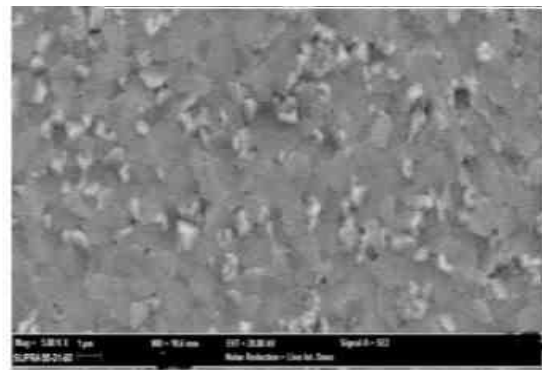


Fig 17: SEM Micrographs of tin at 10X Magnification

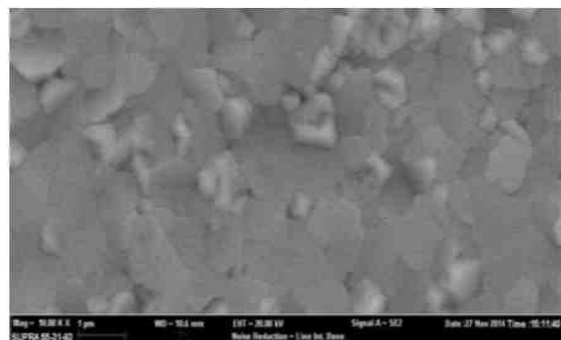


Fig 18: SEM Micrographs of Tin at 25X Magnification

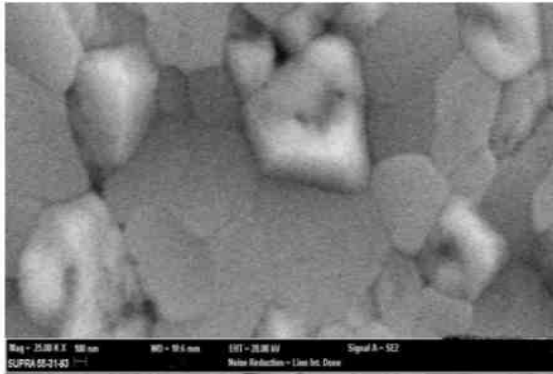


Fig 19: SEM Micrographs of tin at 25X Magnification

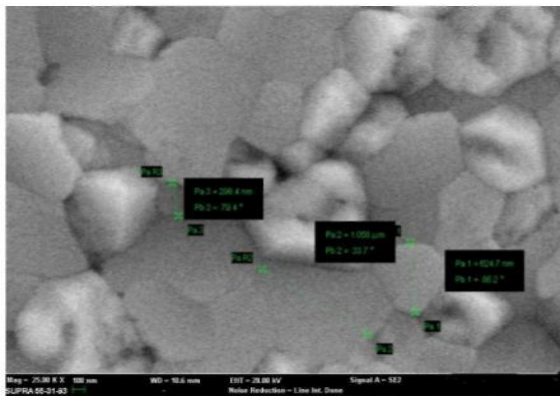


Figure 20, 21 shows the SEM micrographs of Indium deposition on silicon substrate at 5KX, 10KX magnification, 20KV EHT, working distance 8.5mm for study the microstructure and grain size and shows the grain sizes 10-200nm with coarse dispersion on the surface.

Fig 20: SEM Micrographs of Indium-tin at 5X Magnification

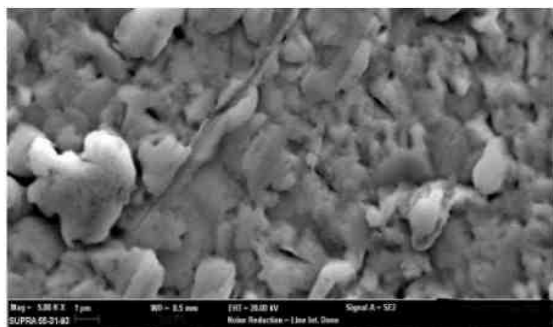


Fig 21: SEM Micrographs of Indium-tin at 10X Magnification

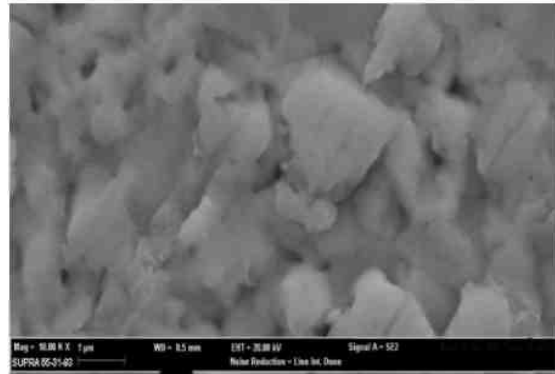
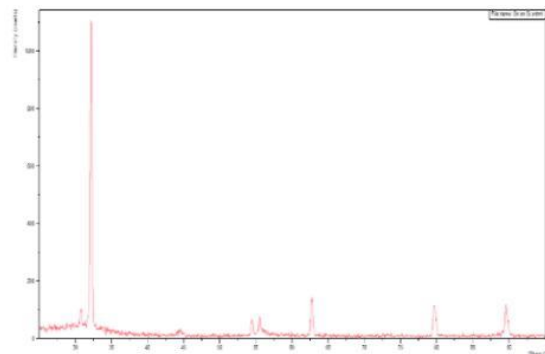


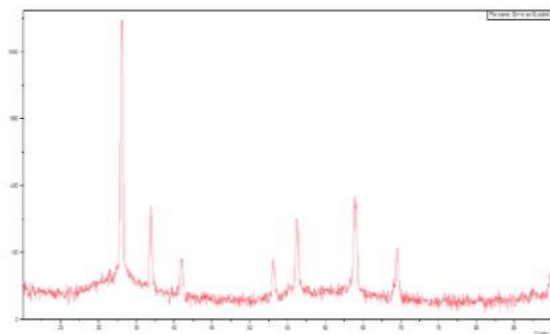
Figure 22 shows the XRD analysis by using Ka (wavelength 1.541874) of tin on silicon which shows that it is polycrystalline structure with multiple peaks at 2θ angle

Fig 22: XRD analysis of tin on silicon



Similarly, the XRD analysis of indium on silicon is shown in figure 23 which shows different peaks of intensity at different 2θ angle revealing the polycrystalline structure.

Fig 23: XRD Analysis of Indium on Silicon



6.0 Conclusion

For Optimized Methods for Fast and Accurate Simulations, gases at low pressures cannot be modeled using conventional computational fluid dynamics tools. That is due to the fact that kinetic effects become important as the mean free path of the gas molecules becomes comparable to the length scale of the flow. Coatings of tin & indium having good uniformity & appropriate thickness have been produced on stationary, non-rotated, flat substrates using a vacuum thermal evaporation technique that incorporates the use of a resistively heated tungsten boat. The thickness uniformity around the substrate was a sensitive function of the mean free path as well as evaporant incidence angle. Also to increase the rate of evaporation we have to raise the temperature of the source. Thus this work presents the thermal evaporation of tin and indium on silicon with thickness of polycrystalline tin 164 nm and indium 182 nm. Also microstructure study at different magnifications show polycrystalline structure for tin and indium which can be transformed to single crystal and uniform grain size across grain boundaries by optimizing deposition rate and conditions. SEM micrographs of tin and indium at different magnifications shows the 100nm to 1 microns grain size along the grain boundaries. Similarly, XRD analysis with $K\alpha$ shows the peaks of intensity at different 2 θ angles for different orientations of planes with polycrystalline structure.

References

- [1] Ali Moarrefzadeh et.al., Simulation and Modeling of Physical Vapor Deposition (PVD) Process, *Wseas Transactions on Applied and Theoretical Mechanics*, 7(2), 2012
- [2] G. H. Gilmer et.al., Thin film deposition: fundamentals and modeling, *Journal of Computational Materials Science* 12, 1998, 354-380
- [3] C. R. Zamarrenoa et al. Optical Fiber Refractometers based on Indium Tin Oxide Coatings with Response in the Visible Spectral Region
- [4] Souad Laghrib et al. , Tin oxide thin layers obtained by vacuum evaporation of tin and annealing under oxygen flow, *Vacuum* 82 (2008) 782-788
- [5] Sea-Way Jan, Si-Chen Lee, Preparation and Characterization of Indium-Tin-Oxide Deposited by Direct Thermal Evaporation of Metal Indium and Tin, *J. Electrochemistry. Soc: Solid State Science and Technology*, 134(8), 1987
- [6] D. Bruce Buchholz et.al, Differences between amorphous indium oxide thin films; *Progress in Natural Science: Materials International*, 23(5), 2013, 475-480
- [7] Alexandra C. Fechete et al., Growth of Indium Oxide Nanostructures by Thermal Evaporation, Sensor Technology lab., RMIT university, Australia, 1-4244-0453-3/06/\$20.00@2006 IEEE
- [8] C. A. Pan, T. P. Ma, High quality transparent conductive indium oxide films prepared by thermal evaporation, *Appl. Phys. Lett.*, American Institute of Physics, 37(2), 1980
- [9] B. Maniscalco, P. M. Kaminski, J. M. Walls, Thin film thickness measurement using Scanning White Light Interferometry, 550, 2014, 10-16
- [10] M. Trzcinski et al, Alloy formation of ultrathin indium and silver layers on W(100): A photoemission study, *Material Science* 589 (2005) 192 -200
- [11] Authur K. Burak Ucer, Vacuum evaporation, www.users.wfu.edu